CrystEngComm

ROYAL SOCIETY OF CHEMISTRY

PAPER

View Article Online
View Journal | View Issue

Check for updates

Cite this: *CrystEngComm*, 2024, **26**, 1701

Cd(II) and Zn(II) coordination polymer-assisted CO_2/cyclohexene oxide copolymerization with a double metal cyanide catalyst†

Zi-Qing Huang,[a] Jia-Qi Chen,[a] Xiao-Yu Zhang,[a] Cheng-Kai Yuan,[a] Peng Wang,[a] Yue Zhao,[a] Bao-Cheng Zhao,*[b] Wei-Xin Qi*[b] and Wei-Yin Sun*[a]

Received 20th December 2023,
Accepted 14th February 2024

DOI: 10.1039/d3ce01289a

rsc.li/crystengcomm

It is attractive but challenging to develop a cocatalyst for CO_2/cyclohexene oxide (CHO) copolymerization with a double metal cyanide (DMC) catalyst. In this study, we synthesized three coordination polymers (CPs) [Cd(3N3PY)(NDC)]·0.58H_2O (**1**), [Zn(3N3PY)(IPA)]·3H_2O (**2**) and [Cd(3N3PY)(NPA)]·2DMF·2H_2O (**3**) (3N3PY = 4′-(4-(1*H*-1,2,4-triazol-1-yl)phenyl)-2,2′:6′,2″-terpyridine, H_2NDC = 2,6-naphthalene dicarboxylic acid, H_2IPA = isophthalic acid, H_2NPA = 2,2′-dinitro-4,4′-biphenyldicarboxylic acid). Crystal structural analyses show that **1–3** are different one-dimensional (1D) chains that further assemble into three-dimensional (3D) supramolecular structures by π–π and hydrogen bonding interactions. CPs **1–3** were applied as cocatalysts to assist DMC for CO_2/CHO copolymerization and the efficient proportion of carbonate $P_{-OC(O)O-}$ in the product is 59% achieved for **2** at 80 °C in 1 MPa CO_2. The proportion of carbonate $F(CO_2)$ and conversion rate of CHO (C_{CHO}) are 63% and 93%, respectively. The mechanistic study on structure–activity relationship and chemoselectivity was performed.

Introduction

Excessive emission of carbon dioxide (CO_2) is one of the main reasons for the greenhouse effect, which is hazardous to the environment and human health.[1] Thus, it is meaningful to develop valid methods to consume the excessive CO_2 in the atmosphere. In fact, CO_2 is a kind of resource-rich, renewable and non-toxic carbon source.[2] As reported previously, the ring opening reaction of epoxides with CO_2 is an efficient and atom-economic way for chemically fixing CO_2.[3] As a result, it is attractive to create effective catalysts and explore valid methods to control the selectivity of products.[4]

In 2020, Hu and Zhang's group synthesized an Al-salen catalyst in cooperation with an ionic liquid to convert CO_2 into cyclic carbonate.[5] The highest yield is 92% with a wide scope of substrates at 25 °C and 1 MPa CO_2. In 2018, Wang's lab reported Al-porphyrin catalysts for copolymerization of CO_2 and propylene oxide (PO).[6] At 80 °C and 4 MPa CO_2, the proportion of carbonate, defined as $F(CO_2)$, in the produced polymer is 53.1% in the obtained PO–CO_2 polyols and the conversion rate of PO is 99%. Recently, the same group studied the copolymerization of CO_2 with cyclohexene oxide (CHO) heterogeneously catalyzed by double metal cyanide (DMC) at 80 °C and 3 MPa CO_2.[7] As a result, the $F(CO_2)$ value is 96% and the conversion rate of CHO is 99%. In the last decades, DMC was found to be efficient for binary and ternary copolymerization with advantages of simple preparation, low synthetic cost and insensitivity to water and air.[8,9] Recyclable aliphatic polycarbonate products have demands in wide applications like environmental protection, adhesives, electronic devices, biomedical materials and automobile accessories.[10,11] In the reported studies, cocatalysts of DMC to enrich the function of products and optimize the reaction conditions are seldom explored.

Owing to the open metal and bifunctional acid–base sites, coordination polymers (CPs) are considered to be desirable for catalysis by forming noncovalent interactions with organic substrates, such as ionic, cation–π, anion–π, lone pair–π, π–π stacking, *etc.*[12,13] Furthermore, in the epoxide and CO_2 atmosphere, CPs are considered to form metal carbonate species, which is derived from control experiments by separately catalysing the CHO/CO_2 reaction with only heat or addition of bis(triphenylphosphine)iminium chloride (PPNCl) or tetrabutylammonium bromide (NBu_4Cl) as a cocatalyst at 80 °C. Besides, the detailed kinetic studies were also conducted and analyzed.[14]

[a] *Coordination Chemistry Institute, State Key Laboratory of Coordination Chemistry, School of Chemistry and Chemical Engineering, Nanjing National Laboratory of Microstructures, Collaborative Innovation Center of Advanced Microstructures, Nanjing University, Nanjing 210023, China. E-mail: sunwy@nju.edu.cn*

[b] *Huaian Bud Polyurethane Science & Technology Co., Ltd., Huaian 223100, China. E-mail: zbc@budpu.com, qwx@budpu.com*

† Electronic supplementary information (ESI) available. CCDC 2314992–2314994. For ESI and crystallographic data in CIF or other electronic format see DOI: https://doi.org/10.1039/d3ce01289a

Based on the above-mentioned situation, in this work, we designed and synthesized three CPs with terpyridyl ligand 4′-(4-(1*H*-1,2,4-triazol-1-yl)phenyl)-2,2′:6′,2″-terpyridine (3N3PY), namely [Cd(3N3PY)(NDC)]·0.58H_2O (**1**), [Zn(3N3PY)(IPA)]·3H_2O (**2**) and [Cd(3N3PY)(NPA)]·2DMF·2H_2O (**3**) (H_2NDC = 2,6-naphthalene dicarboxylic acid, H_2IPA = isophthalic acid, H_2NPA = 2,2′-dinitro-4,4′-biphenyldicarboxylic acid). They were applied as cocatalysts for CO_2/CHO copolymerization with DMC. It was found that the efficient carbonate proportion was achieved with the assistance of CPs and the mechanism was also explored.

Experimental

Materials and general methods

All commercially available solvents and chemicals are of reagent grade and were used directly without further purification. DMC solvent with the formula $Zn_3[Co(CN)_6]_2$·$ZnCl_2$·solvent is a commercial product of Huaian Bud Polyurethane Science & Technology Co., Ltd. Ligand 3N3PY was prepared according to the previously reported method.[15–17] Powder X-ray diffraction (PXRD) data were collected on a Bruker D8 Advance X-ray diffractometer with Cu Kα (λ = 1.5418 Å) radiation. Thermogravimetric analysis (TGA) was carried out on a Mettler-Toledo (TGA/DSC1) thermal analyzer with a heating rate of 10 °C min^{-1} under a N_2 atmosphere. FTIR-ATR spectra were measured on a Bruker Tensor II infrared spectrophotometer equipped with a diamond ATR module in the range of 400–4000 cm^{-1}. Elemental analyses for C, H and N were performed on an Elementar Vario MICRO elemental analyzer. ^{1}H NMR spectra were recorded on a Bruker-DRX instrument (500 MHz).

Synthesis of [Cd(3N3PY)(NDC)]·0.58H_2O (1)

A mixture of 3N3PY (18.82 mg, 0.05 mmol), H_2NDC (10.81 mg, 0.05 mmol) and $Cd(NO_3)_2$·4H_2O (15.40 mg, 0.05 mmol) in a mixed solvent of DMF/H_2O (2 mL, v : v = 3 : 1) was charged into a 10 mL glass vial, and then heated at 110 °C for 72 h under solvothermal conditions. The yield of the obtained crystals was 25% after cooling down to ambient temperature. FTIR-ATR (cm^{-1}, Fig. S1†): 3658 (w), 3099 (w), 2983 (w), 2897 (w), 1662 (w), 1606 (m), 1551 (m), 1470 (w), 1400 (s), 1350 (m), 1284 (w), 1239 (w), 1143 (w), 1088 (w), 1052 (w), 1011 (w), 979 (w), 915 (w), 841 (w), 787 (s), 734 (m), 670 (m), 627 (m), 520 (w), 488 (w), 446 (m).

Synthesis of [Zn(3N3PY)(IPA)]·3H_2O (2)

$Zn(NO_3)_2$·6H_2O (14.88 mg, 0.05 mmol), 3N3PY (18.82 mg, 0.05 mmol), H_2IPA (8.31 mg, 0.05 mmol) and 2 mL DMF/H_2O (v : v = 3 : 1) mixed solvent were added into a 10 mL glass vial. Then, it was heated at 110 °C for 72 h. After cooling to room temperature, colorless crystals were obtained with a yield of 68%. FTIR-ATR (cm^{-1}, Fig. S1†): 3483 (w), 3062 (w), 1676 (w), 1609 (s), 1554 (m), 1530 (m), 1473 (m), 1405 (m), 1337 (s), 1147 (w), 1085 (w), 1011 (w), 977 (w), 834 (w), 793 (m), 749 (m), 725 (m), 660 (w), 569 (w), 521 (w), 420 (w).

Synthesis of [Cd(3N3PY)(NPA)]·2DMF·2H_2O (3)

A mixture of $Cd(NO_3)_2$·4H_2O (15.40 mg, 0.05 mmol), 3N3PY (18.82 mg, 0.05 mmol), H_2NPA (16.61 mg, 0.05 mmol) and 2 mL DMF/H_2O (v : v = 3 : 1) mixed solvent in a 10 mL glass vial was heated at 110 °C for 72 h. After cooling to room temperature, yellow block crystals were obtained with a yield of 58%. FTIR-ATR (cm^{-1}, Fig. S1†): 3427 (w), 3104 (w), 2923 (w), 2862 (w), 1666 (s), 1597 (s), 1526 (s), 1481 (m), 1390 (s), 1345 (s), 1279 (m), 1240 (m), 1153 (w), 1086 (m), 1007 (m), 970 (m), 916 (m), 835 (m), 785 (s), 724 (m), 669 (m), 512 (m), 482 (w), 421 (m).

Synthesis of methyl iodized CPs 1Me–3Me

The methyl iodized CPs were prepared with modification of the previously reported method.[18] CP **1** (20 mg, 0.028 mmol)/**2** (20 mg, 0.030 mmol)/**3** (20 mg, 0.020 mmol), 4 mL DMF and 48 μL (0.77 mmol) methyl iodide (CH_3I) were added into a glass vial. Then, the mixture was heated at 70 °C for 12 h. After cooling, the obtained product was added to 15 mL ethyl acetate and the precipitate was collected by filtration. After washing with diethyl ether and vacuum drying, the final products **1**Me/**2**Me/**3**Me were obtained.

Catalytic copolymerization of the CO_2/CHO reaction with DMC and 1–3

5 mg DMC, 3.5 μmol activated CP obtained by heating at 230 °C in vacuum for 12 h and 0.5 mL CHO were added into a Teflon-lined stainless steel container. Then, CO_2 gas was charged and pressurized at 1 MPa. The sealed reactor was heated at 80 °C using an oil bath for 12 h. After cooling to room temperature, CO_2 gas was slowly released and the obtained product was determined by ^{1}H NMR in $CDCl_3$.

Results and discussion

Crystal structure description

Crystal structure of [Cd(3N3PY)(NDC)]·0.58H_2O (1). Single crystal X-ray diffraction results are presented in Fig. 1. The space group of **1** is $P2_1/c$ belonging to the monoclinic crystal system (Table 1). The central Cd(II) coordinates with four oxygen atoms (O1, O2, O3 and O4) from two NDC^{2-} and three nitrogen atoms (N1, N2 and N3) from one 3N3PY (Fig. 1a). The bond lengths of Cd–O and Cd–N are in the range of 2.2988(17)–2.5525(17) Å and 2.3372(18)–2.407(2) Å, respectively (Table S1†). The Cd(II) atoms are linked together by NDC^{2-} ligands to form an infinite one-dimensional (1D) chain, in which 3N3PY serves as the terminal ligand (Fig. 1b). The 1D chains are further assembled into a three-dimensional (3D) supramolecular structure (Fig. S2a†) through π–π interactions between the 3N3PY moieties (Fig. 1c, Tables S2 and S3†). In addition, there are C–H···O hydrogen bonds between the C–H bond in 3N3PY and the

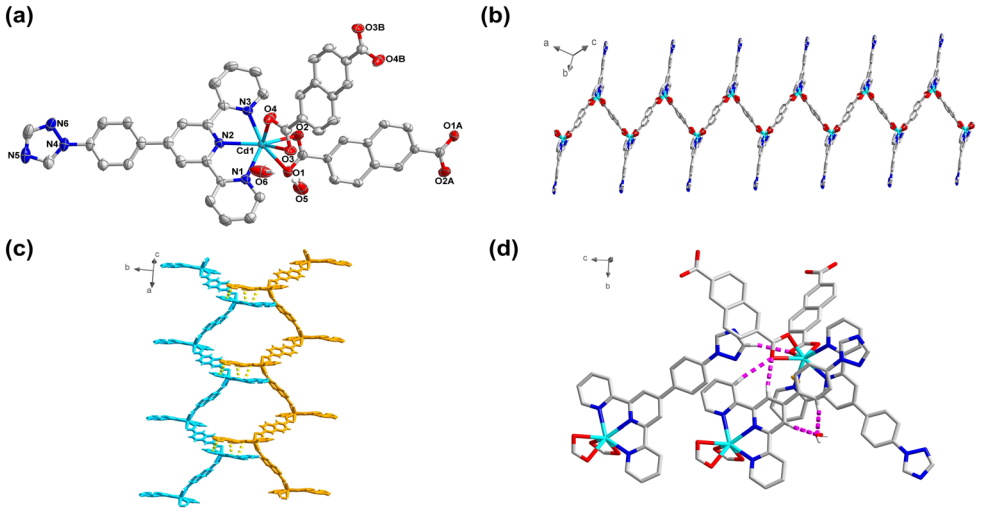

Fig. 1 (a) Coordination environment of Cd(II) in **1** with the ellipsoids drawn at the 50% probability level. Hydrogen atoms are omitted for clarity. (b) 1D chain in **1**. (c) Selected π–π interactions in **1**. (d) Hydrogen bonds in **1**.

Table 1 Crystal data and structure refinements for **1–3**

Compound	**1**	**2**	**3**
Formula	$C_{35}H_{23.17}N_6O_{4.58}Cd$	$C_{31}H_{26}N_6O_7Zn$	$C_{43}H_{40}N_{10}O_{12}Cd$
Formula weight	713.48	659.95	1001.25
Temperature (K)	296.15	193	193
Crystal system	Monoclinic	Triclinic	Tetragonal
Space group	$P2_1/c$	$P\bar{1}$	$P4_12_12$
a (Å)	10.6395(3)	8.8685(9)	18.1361(9)
b (Å)	28.9664(8)	10.2782(11)	18.1361(9)
c (Å)	10.5656(4)	16.752(2)	26.421(2)
α (°)	90	95.095(7)	90
β (°)	114.3410(10)	101.142(6)	90
γ (°)	90	110.208(5)	90
V (Å^3)	2966.74(16)	1385.8(3)	8690.2(11)
Z	4	2	8
Dc (g cm^{-3})	1.597	1.582	1.531
μ (mm^{-1})	0.791	1.153	3.154
F(000)	1439	680	4096
Data collected	23 532	4858	82 863
Unique reflections	5491	4858	7974
Goodness-of-fit	1.060	1.041	1.034
$R_1{}^a$ [$I > 2\sigma(I)$]	0.0279	0.0967	0.0314
w$R_2{}^b$ [$I > 2\sigma(I)$]	0.0646	0.2581	0.0795

^{a} $R_1 = \sum||F_o| - |F_c||/\sum|F_o|$. ^{b} $wR_2 = |\sum w(|F_o|^2 - |F_c|^2)|/\sum|w(F_o)^2|^{1/2}$, where $w = 1/[\sigma^2(F_o{}^2) + (aP)^2 + bP]$. $P = (F_o{}^2 + 2F_c{}^2)/3$.

oxygen atoms in the carboxylate group of NDC^{2-} as well as the non-coordinated water molecule (Fig. 1d). The detailed hydrogen bonding data are summarized in Table S4.†

Crystal structure of [Zn(3N3PY)(IPA)]·3H$_2$O (2). The space group of crystal **2** is $P\bar{1}$ in the triclinic crystal system, which is distinct from that of **1** (Table 1). The asymmetric unit of **2** consists of one Zn(II), one 3N3PY and one IPA^{2-}. Zn(II) exhibits a five-coordinated environment and is surrounded by three nitrogen atoms N1, N2 and N3 from one 3N3PY and two oxygen atoms O3 and O1A [symmetry code: $(x, -1 + y, z)$] from two different IPA^{2-} (Fig. 2a) with normal Zn–N and Zn–O bond distances (Table S1†). Each IPA^{2-} coordinates with two Zn(II) atoms to form 1D chains (Fig. 2b), which are further connected with each other to form a 3D supramolecular structure (Fig. S2b†) by π–π interactions between two neighbouring 3N3PY ligands (Fig. 1c, Tables S2 and S3†) and hydrogen bonds like C(9)–H(9)···N(6) (2.44 Å), C(12)–H(12)···O(4) (2.25 Å) and C(20)–H(20)···O(2) (2.36 Å) (Fig. 1d and Table S4†). It is noteworthy that the 1D chain in **1** stretches as a zigzag-type with terminal 3N3PY ligands bidirectionally arranged (Fig. 1b), while in **2** the 1D chain is linear and the 3N3PY ligands arrange in one direction (Fig. 2b).

Crystal structure of [Cd(3N3PY)(NPA)]·2DMF·2H$_2$O (3). CP **3** was isolated with a similar preparation method to **1** by changing the carboxylic acid ligand to H_2NPA instead of

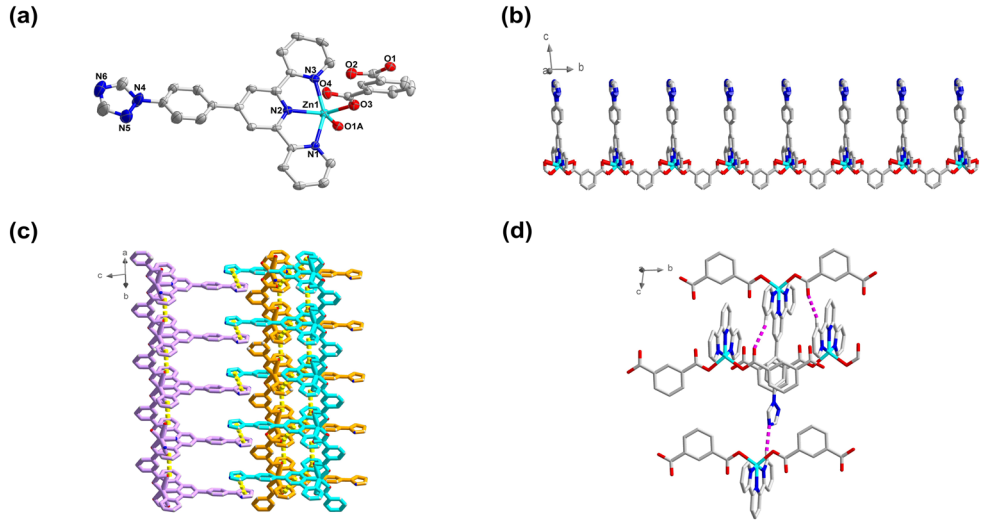

Fig. 2 (a) Coordination environment of Zn(II) in **2** with the ellipsoids drawn at the 50% probability level. Hydrogen atoms are omitted for clarity. (b) 1D chain in **2**. (c) Selected π–π interactions in **2**. (d) Hydrogen bonds in **2**.

H_2NDC. The results of crystal structural analysis revealed that **3** crystallizes in the tetragonal crystal system with a chiral space group of $P4_12_12$ [the Flack factor is 0.058(9)], which is different from **1** and **2** (Table 1). The asymmetric unit of **3** contains one Cd(II) ion, one 3N3PY and one NPA^{2-} ligand. Each Cd(II) atom connects three nitrogen atoms N1, N2 and N3 derived from the terpyridyl unit in 3N3PY and three oxygen atoms O1, O7A and O8A [symmetry code: $(-x, 1 - y, -0.5 + z)$] from two carboxylate groups of different NPA^{2-} ligands (Fig. 3a). Each dicarboxylate NPA^{2-} ligand connects two Cd(II) to form a 1D chain (Fig. 3b). The helical chiral structure may arise from the spiral twist of the dinitrobiphenyl moieties in NPA^{2-}.[17] The 1D chains are further connected by π–π interactions between the neighbouring 3N3PY (Fig. 3c, Tables S2 and S3†) and hydrogen bonds C–H···O (Fig. 3d and Table S4†) to assemble into a 3D structure (Fig. S2c†).

Characterization of 1–3

IR spectra of **1–3** and ligands are shown in Fig. S1† and no vibrational bands were observed between 1680 and 1760 cm^{-1} for the synthesized **1–3**, implying the complete deprotonation of the dicarboxylic acid to produce a dicarboxylate ligand coordinating with the metal centers in **1–3**. This is in good agreement with the results of crystal structure analysis as mentioned above. The measured PXRD patterns of the as-synthesized **1–3** are consistent with the simulated results from the single crystal structure analysis (Fig. S3†), indicating the good crystallinity and phase purity of the bulky samples **1–3**. As shown in Fig. S4,† thermogravimetric (TG) data reflect the thermal stability of **1–3**. The weight loss of solvent molecules mainly occurred from 25 to 180 °C with 1.39% for **1** and 8.82% for **2**, which are consistent with the theoretical results of 1.46% for **1** and

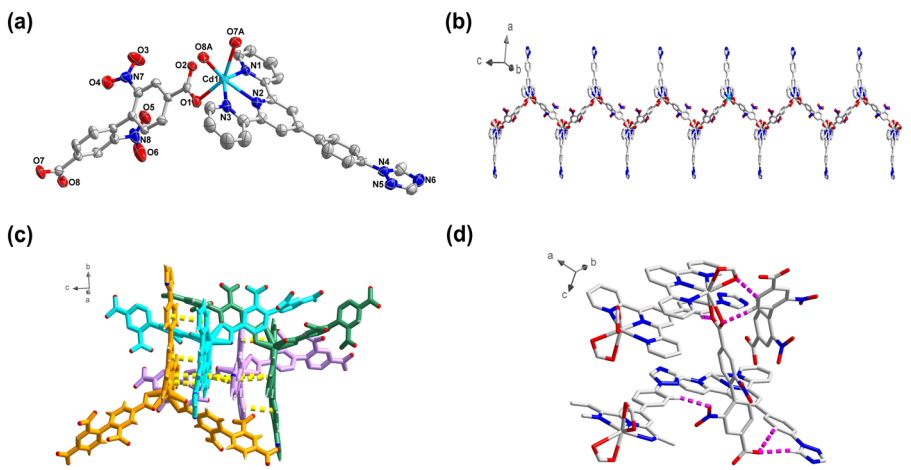

Fig. 3 (a) Coordination environment of Cd(II) in **3** with the ellipsoids drawn at the 50% probability level. Hydrogen atoms are omitted for clarity. (b) 1D chain in **3**. (c) Selected π–π interactions in **3**. (d) Hydrogen bonds in **3**.

8.21% for **2**. Further, the collapse of the 3D supramolecular framework starts from 390 °C. For **3**, the weight decreased by 16.65% in the range of 25–247 °C, which is caused by the loss of DMF and water molecules with a theoretical value of 18.18%. CP **3** maintained stable at 247–308 °C and then the structure began to decompose.

Catalytic copolymerization of CO_2/CHO by DMC and 1–3

It has been proved that the ring opening reaction of epoxide with CO_2 is an effective approach to the chemical fixation of CO_2. Accordingly, CPs **1**, **2** and **3** were utilized to cocatalyze CO_2/CHO copolymerization with DMC. According to the ^{1}H NMR data of the product, the wide signals in 3.26–3.75 and 4.32–4.80 ppm indicate that the copolymers were obtained and CO_2 was fixed into the copolymers as a carbonate group. The proportion of carbonate in the obtained copolymer is recorded as the $F(CO_2)$ value and C_{CHO} indicates the conversion rate of CHO, while $P_{-OC(O)O-}$ means the proportion of carbonate in the total product, and $P_{-OC(O)O-} = F(CO_2) \times C_{CHO}$.

In this study, CPs **1**, **2**, and **3** with Zn(II) and Cd(II) with d^{10} electron configuration were applied to cocatalyze the CO_2/CHO reaction with DMC at 80 °C. The $F(CO_2)$ values are 65%, 63% and 60% for CPs **1**, **2** and **3**, respectively, which are significantly improved comparing with the result of 47% for sole DMC without CPs (Fig. 4 and Table 2). The C_{CHO} values are 90%, 93% and 94% for CPs **1**, **2** and **3**, respectively, while it was 76% in the absence of cocatalysts **1**, **2**, and **3**. The total carbonate groups existing in the product $P_{-OC(O)O-}$ are 58%, 59% and 56% for CPs **1**, **2** and **3**, respectively, and these values are obviously improved by comparing with the result of 36% without CPs (Table 2).

Owing to the specific structure of the obtained CPs, the non-coordinated free triazole may influence the ability of adsorbing CO_2 in the reaction. In order to further verify this conjecture, the triazole was methylated and the NMR spectra

Table 2 DMC assisted with CPs **1**–**3** and **1**Me–**3**Me for CO_2/CHO copolymerization[a]

Cocatalyst	$F(CO_2)$/%	C_{CHO}/%	$P_{-OC(O)O-}$/%
1	65	90	58
2	63	93	59
3	60	94	56
1Me	51	22	11
2Me	62	31	19
3Me	68	74	50
None	47	76	36
$Cd(OAc)_2$	35	98	34
PhCOONa	<1	<1	<1
3N3PY	<1	<1	<1

[a] Reaction conditions: DMC (5 mg), cocatalyst (3.5 μmol), CHO (0.5 mL) at 80 °C, 1 MPa. The results were determined by ^{1}H NMR in $CDCl_3$.

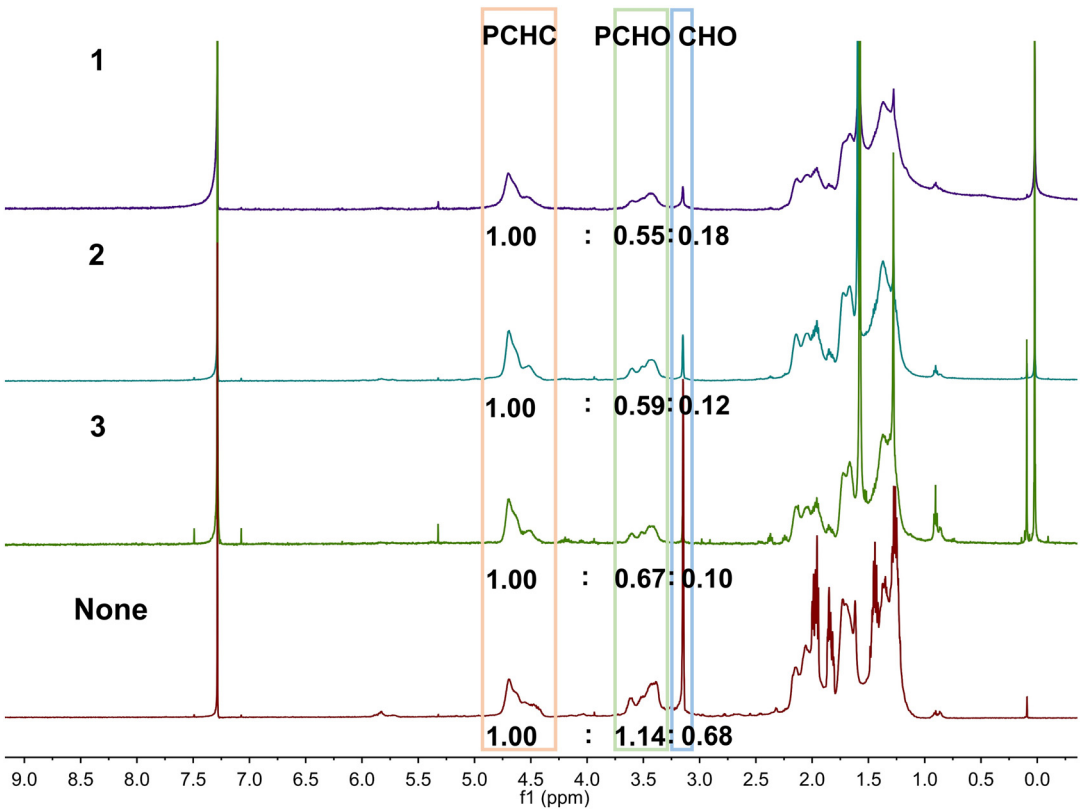

Fig. 4 ^{1}H NMR spectra ($CDCl_3$, 500 MHz) of the products by the addition of CPs **1**–**3**.

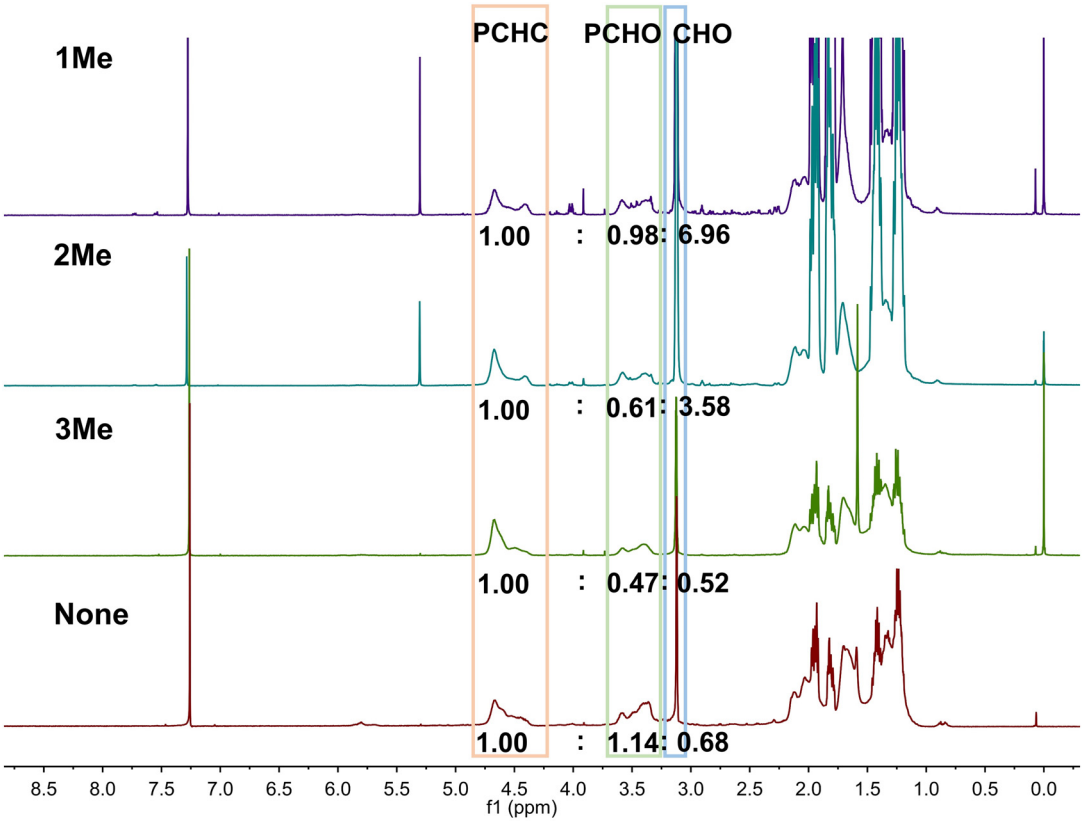

Fig. 5 The ^{1}H NMR spectra ($CDCl_3$, 500 M) of the products by adding CPs **1**Me–**3**Me.

show the complete methylation of the triazole groups in the obtained products **1**Me, **2**Me and **3**Me (Fig. S5–S7†). Then, they were utilized to cocatalyze the CO_2/CHO copolymerization. The ^{1}H NMR data of the products are shown in Fig. 5. After the addition of methylated CPs **1**Me, **2**Me and **3**Me, the $F(CO_2)$ values in the produced copolymers are 51%, 62% and 68%, respectively (Table 2). Meanwhile, the calculated C_{CHO} values are separately 22%, 31% and 74%, and the $P_{-OC(O)O-}$ values are 11%, 19% and 50% for CPs **1**Me, **2**Me and **3**Me, which obviously decreased by comparing with the corresponding results of CPs **1**, **2** and **3** (Table 2). The results imply the role of uncovered free triazoles. Furthermore, C_{CHO} was gradually decreased with the sequence **3**Me, **2**Me and **1**Me. As was reported, the methylated triazole may be able to adsorb CHO as a guest.[18] As shown in Fig. S2,† the overall structure (1D chain) may be beneficial to uncovering triazole groups, which may be suitable for adsorbing CO_2 during the copolymerization.[22] And the carboxylate ligand of the CPs may affect the stacking arrangement of triazole groups in 3N3PY. In CP **1**, ligand 3N3PY is almost perpendicular to each other, while the triazole groups in 3N3PY are presented as head-to-head in CP **2**. In CP **3**, the presence of nitro groups may influence the electron configuration of triazoles by d–π interactions.[19]

Furthermore, control experiments were carried out to test the significance of assembling the d^{10} metal ion(II), carboxylate ligand and terpyridine for cocatalyzing the CO_2/CHO reaction and the results are summarized in Table 2. When $Cd(OAc)_2$ was used as the cocatalyst, the $F(CO_2)$ value for the produced polymer is 35% and C_{CHO} is 98%. However, almost no copolymerization occurred when PhCOONa or 3N3PY was added.

It has been reported that an onium salt with an N-containing functional group is helpful for catalyzing the ring opening reaction of epoxide with CO_2, and NBu_4Br is the popular one for synthesizing cyclic carbonate (Fig. S8†).[20–23] However, in order to fix CO_2 into more valuable and stable polycarbonate, PPNCl is more suitable to alter the selectivity of the product (Fig. 6). In the tests of adding CP **1**/**2**/**3** and PPNCl, the calculated results of $F(CO_2)$ values are separately 71%, 72% and 74%, which are much better than the value of 44% in the absence of CPs (Table 3). Based on the above experimental results, it is speculated that it may result from the combination of the CPs and PPN^+ to form an intermediate, which can adsorb CO_2 and promote the generation of carbonate. However, as for the conversion rate of CHO, it was 81%, 58% and 49% in the presence of CPs **1**, **2** and **3**, respectively, and it was 89% for the sample without adding CPs. It is obvious that CP **1** presents a more efficient result for fixing CO_2. Owing to similar Lewis acidic electronic effects of DMC, CPs **1**–**3** and PPN^+, competition may occur and hinder the contact between the epoxy group in CHO and catalytic sites on DMC when PPNCl and CPs were added. The comparison with other reported systems is listed in Table

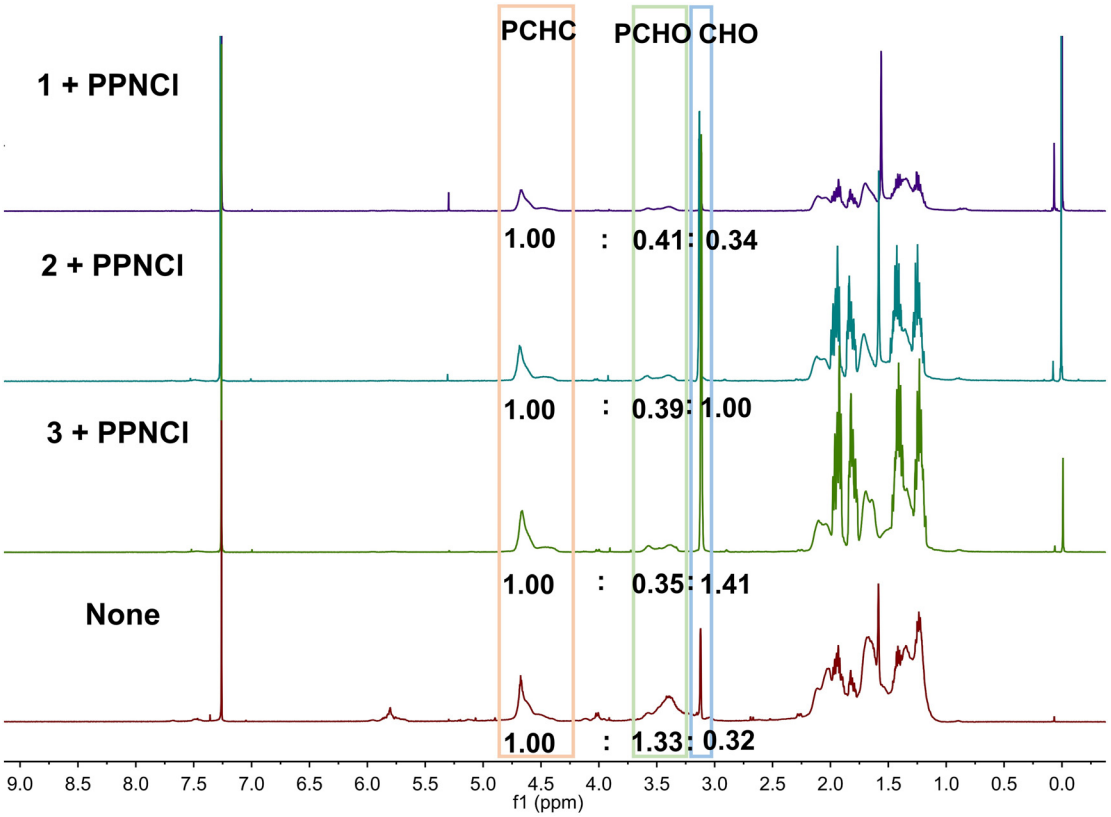

Fig. 6 ^{1}H NMR spectra ($CDCl_3$, 500 MHz) of the products by adding PPNCl and CPs **1**–**3**.

S5,† and it presents a preferable result for fixing CO_2 into a carboxylate polymer with the assistance of CPs at a low pressure of CO_2.

Kinetic analysis of the CO_2/CHO reaction catalyzed by CPs 1–3 and DMC

As shown above, CPs give superior cocatalytic performance for CO_2/CHO copolymerization and **2** is used as an example for kinetic analysis characterized by ^{1}H NMR. It is obvious that in the early stage of the reaction, the concentration of the substrate decreased linearly with time, indicating that the ring opening of CHO was a zero-order reaction. And the reaction rate constants are separately 3.19×10^{-6}, 6.94×10^{-6}, 1.49×10^{-5}, and 1.31×10^{-4} s^{-1} with different concentrations of the catalyst (DMC and CP **2**) at 50, 25, 12.5 and 8.3 mM (Fig. S9a–d†). Subsequently, plotting the logarithm of the observed rate coefficient *vs.* the logarithm of the catalyst concentration shows a linear fit between 50 and 12.5 mM, indicating a first order in the catalyst concentration (Fig. S9e†). The rate dependence on CO_2 pressure was determined by measuring the observed rate coefficient over a range of CO_2 pressure from 6 to 10 bar. And the obtained k values are separately 4.70, 6.51, and 3.43×10^{-5} s^{-1} at the pressures of 10, 8, and 6 bar (Fig. S10a–c†).The plot of the rate coefficient *vs.* pressure resulted in a slightly curved fit to the data, but without significant rate changes over the range of 6–10 bar, indicating the zero-order of CO_2 concentration (Fig. S10d†). Therefore, the reaction proceeded in the first-order rate law: first order in the concentration of the catalyst and zero order in CO_2 and single substrate CHO with the rate expression of rate = $[CHO]^0[CO_2]^0[Cat]^1$.

Next, the pressure of CO_2 was considered to be the characterization of dynamic analysis for calculating the activation energy. As shown in Fig. S11,† the calculated rate constants are 0.413, 1.22, 4.70, and 1.82×10^{-5} s^{-1} respectively for 313, 333, 353 and 373 K. It is obvious that the reaction rate gradually increased at 313–353 K, but decreased at 373 K, which is probably induced from the entropy reduction of the reaction and the decomposition of the generated carbonate group at high temperature. In Fig. S12a,† a plot of $\ln(k/T)$ *vs.* $1/T$ was obtained to determine the transition state enthalpy ΔH of 52.90 kJ mol^{-1} and ΔS of −84.32 J mol^{-1} K^{-1} according to the Eyring analysis, *i.e.* overall, the transition state Gibbs free energy was determined

Table 3 DMC assisted with PPNCl and CPs **1**–**3** for CO_2/CHO copolymerization

Cocatalyst	$F(CO_2)$/%	C_{CHO}/%	$P_{-OC(O)O-}$/%
PPNCl + **1**	71	81	58
PPNCl + **2**	72	58	42
PPNCl + **3**	74	49	36
PPNCl	44	89	39

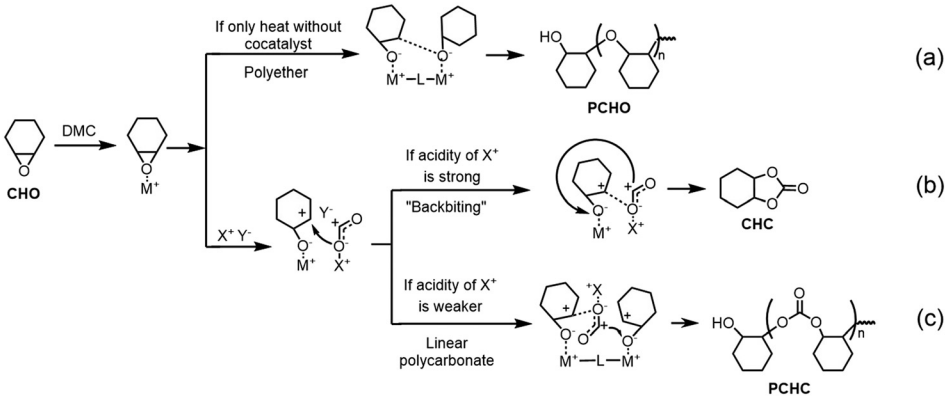

Fig. 7 Proposed mechanism of the chemoselectivity for the CO_2/CHO reaction. (a) PCHO path. (b) CHC path. (c) PCHC path.

as ΔG = 82.66 kJ mol^{-1} (80 °C). Besides, the simple activation energy value (E_a) was also determined as 55.66 kJ mol^{-1} by Arrhenius methods (Fig. S12b†), which may be a preferable method to compare the efficiency of the catalyst for the CO_2/CHO reaction.

Proposed catalytic mechanism

Based on the above data, the selectivity of the CO_2/CHO reaction is considered. It is proposed that the double metal centers of DMC would like to act as the Lewis acid sites to activate epoxide through M–O coordination. As shown in path a (Fig. 7), if the reaction is only heated at 1 bar CO_2 without a cocatalyst, the coordinated oxygen atom will connect with C^+ generated at the adjacent metal in DMC and produce polycyclohexyl ether (PCHO). While, CO_2 was inclined to insert into the M–O bond with the addition of ionic cocatalyst in 1 MPa CO_2, because anion is known to be a good leaving group and always used as initiator.[20,21] Therefore, two halide salts with different onium cations separately participated in the CO_2/CHO reaction with DMC, and the chemoselectivity is obviously altered, which is supposed to be ascribed to the different electrophilic characters of the cations under the reaction conditions. Firstly, the cyclic carbonate was produced with the assistance of NBu_4Cl due to its strong electrophilicity (Fig. 7, path b). In this process, the metal-activated CHO connects with CO_2 and the metallic-carbonate active species perform "back-biting" to produce the five-membered ring by the S_N2 pathway. And in the process of adding PPNCl with weak electrophilicity, the metallic-carbonate preferred to interact with the epoxide group activated at the adjacent metal in DMC and generated the linear polycarbonate (Fig. 7, path c).

In this work, the electrophilicity of CPs **1**–**3** may be similar to that of PPN^+ applied to fix CO_2 into the metallic-carbonate intermediate and produce linear poly(cyclohexene carbonate), which is probably supported with the phenomenon of the low $F(CO_2)$ values when competitive CPs and PPNCl exist simultaneously. Besides, it is interesting that according to the superior catalytic result of CP **2**, the CP with a Zn(II) ion may be more suitable for fixing CO_2 than that with Cd(II) by producing metal–ligand (M–L) active sites due to the high Lewis acidity of Zn(II).[24]

Conclusions

In this work, three novel coordination polymers were synthesized by using Zn(II) and Cd(II) as the metal centers. The ligands were dicarboxylate and N-donor ligand 3N3PY containing a tripyridine group. Then, the obtained CPs **1**–**3** can assist DMC for catalyzing CO_2/CHO copolymerization. The efficient carbonate proportion was obtained with the assistance of **2**, in which the $F(CO_2)$ and C_{CHO} values are separately 72% and 58%. By comparing with the results of the catalysis by the sole metal salts and ligands, the efficiency increased after assembling into CPs. Besides, the dynamic analysis of this first-order reaction was also performed and the ΔG value of the transition state was calculated to be 82.66 kJ mol^{-1} at 80 °C. The simple activation energy value (E_a) was 55.66 kJ mol^{-1}. Furthermore, the mechanism was also tested. It is supposed that the uncovered triazoles in the CPs may be helpful for fixing CO_2, and the chemoselectivity of the CO_2/CHO reaction is probably related to the electrophilicity of cocatalysts.

Conflicts of interest

There are no conflicts to declare.

Acknowledgements

We gratefully acknowledge the National Natural Science Foundation of China (grant no. 22231006 and 22171131). This work was also supported by a project funded by the Priority Academic Program Development of Jiangsu Higher Education Institutions.

Notes and references

1 J. Liu, G. Yang, Y. Liu, D. Wu, X. Hu and Z. Zhang, *Green Chem.*, 2019, **21**, 3834–3838.

2 X. B. Lu and D. J. Darensbourg, *Chem. Soc. Rev.*, 2012, **41**, 1462–1484.
3 G. Trott, J. A. Garden and C. K. Williams, *Chem. Sci.*, 2019, **10**, 5851–5852.
4 C. Zhuo, H. Cao, H. You, S. Liu, X. Wang and F. Wang, *ACS Macro Lett.*, 2022, **11**, 941–947.
5 J. Liu, G. Yang, Y. Liu, D. Zhang, X. Hu and Z. Zhang, *Green Chem.*, 2020, **22**, 4509–4515.
6 C. Zhuo, H. Cao, X. Wang, S. Liu and X. Wang, *Chin. Chem. Lett.*, 2023, **34**, 108011.
7 W. Mo, C. Zhuo, S. Liu, X. Wang and F. Wang, *Polym. Chem.*, 2023, **14**, 152–160.
8 I. Kim, M. J. Yi, K. J. Lee, D. W. Park, B. U. Kim and C. S. Ha, *Catal. Today*, 2006, **111**, 292–296.
9 A. Peeters, P. Valvekens, R. Ameloot, G. Sankar, C. E. A. Kirschhock and D. E. De Vos, *ACS Catal.*, 2013, **3**, 597–607.
10 P. Wei, G. A. Bhat and D. J. Darensbourg, *Angew. Chem., Int. Ed.*, 2023, e202307507.
11 S. Z. Islam, D. S. Sholl, J. A. Steckel and R. L. Thompson, *Process Saf. Prog.*, 2023, **42**, 371–376.
12 Y. S. Kang, Y. Lu, K. Chen, Y. Zhao, P. Wang and W. Y. Sun, *Coord. Chem. Rev.*, 2019, **378**, 262–280.
13 A. V. Gurbanov, F. I. Guseinov, M. Fátima and C. Guedes da Silva, *Coord. Chem. Rev.*, 2019, **387**, 32–46.
14 P. K. Saini, C. Romaina and C. K. Williams, *Chem. Commun.*, 2014, **50**, 4164–4167.
15 P. Wang, Z. Li, G. C. Lv, H. P. Zhou, C. Hou, W. Y. Sun and Y. P. Tian, *Inorg. Chem. Commun.*, 2012, **18**, 87–91.
16 P. Wang, L. Luo, T. Okamura, H. P. Zhou, W. Y. Sun and Y. P. Tian, *Polyhedron*, 2012, **44**, 18–27.
17 P. Wang, T. Okamura, H. P. Zhou, W. Y. Sun and Y. P. Tian, *Chin. Chem. Lett.*, 2013, **24**, 20–22.
18 Y. L. Liu, Z. H. Huang, X. X. Tan, Z. Q. Wang and X. Zhang, *Chem. Commun.*, 2013, **49**, 5766–5768.
19 M. Kurihara and H. Nishihara, *Coord. Chem. Rev.*, 2002, **226**, 125–135.
20 Z. Su, M. S. Chen, J. Fan, M. Chen, S. S. Chen, L. Luo and W. Y. Sun, *CrystEngComm*, 2010, **12**, 2040–2043.
21 B. W. Jiang, J. Liu, W. J. Xiong, M. L. Weng, J. G. An, Y. W. Fan, L. Z. Zheng, G. Q. Yang and Z. B. Zhang, *Chem. Eng. J.*, 2023, **476**, 146873.
22 D. Zhao, X. H. Liu, Z. Z. Shi, C. D. Zhu, Y. Zhao, P. Wang and W. Y. Sun, *Dalton Trans.*, 2016, **45**, 14184.
23 C. J. Zhang, S. Q. Wu, S. Boopathi, X. H. Zhang, X. Hong, Y. Gnanou and X. S. Feng, *ACS Sustainable Chem. Eng.*, 2020, **8**, 13056–13063.
24 F. Guo, R. X. Li, S. Z. Yang, X. Y. Zhang, H. J. Yu, J. J. Urban and W. Y. Sun, *Angew. Chem., Int. Ed.*, 2023, **62**, e202216232.